Journal of Magnetism and Magnetic Materials 484 (2019) 451–455

Contents lists available at ScienceDirect

Journal of Magnetism and Magnetic Materials

journal homepage: www.elsevier.com/locate/jmmm

Research articles

Twisted skyrmions through dipolar interactions

S. Castillo-Sepúlveda[a], R.M. Corona[b,d], A.S. Núñez[c,d], D. Altbir[b,d,*]

[a] Departamento de Ingeniería, Universidad Autónoma de Chile, Avda. Pedro de Valdivia 425, Providencia, Chile
[b] Departamento de Física, Universidad de Santiago de Chile, USACH, Avda. Ecuador 3493, Estación Central, Santiago, Chile
[c] Departamento de Física, Facultad de Ciencias Físicas y Matemáticas, Universidad de Chile, Casilla 487-3, Santiago, Chile
[d] Center for the Development of Nanoscience and Nanotechnology, CEDENNA, Avda. Libertador Bernardo O'Higgins 3363, Estación Central, Santiago, Chile

A B S T R A C T

The manifestations of the dipolar interaction in magnetic nano-devices can take subtle forms. In this work, we address the effects of dipolar interactions on skyrmions textures. The so-called twisted skyrmion is a natural state between the Bloch skyrmion, that arises from the bulk-like Dzyalonshinskii-Moriya (DM) interaction, and the Néel-skyrmion, that results from the interfacial form of the DM interaction. Often neglected, or approximated by local interactions, we show how, when explicitly included, dipolar interactions generate gaps in the phase diagram for certain helicities. Besides, this interaction allows the existence of skyrmions with two chiralities, which are unstable when the dipolar interaction is approximated by a shape anisotropy.

1. Introduction

Recently magnetic skyrmions [1,2] have been intensely studied from the theoretical [3,4] and experimental [5–7] perspectives. Among their characteristics, one can highlight their small size, their stability under external disturbances, and the possibility of controlling their position with ultra low current densities. Due to these properties, among others, such magnetic configurations offer potential applications in information storage and processing devices [8–12]. Within the family of skyrmions-like magnetic textures, there are two structures that have concentrated most of the attention, namely the Néel and Bloch skyrmions [13,14]. The Néel skyrmion is also known as hedgehog skyrmion, and has a radial magnetization different from zero, while the Bloch skyrmion presents a magnetic texture similar to a vortex, but instead of having only one section, it has two regions in which the magnetization points out of the plane. However, similar to what happens with magnetic vortices [15], Néel and Bloch skyrmions are two extremes of a whole continuous range of possible intermediate states.

It is well known that skyrmions can be obtained in thin magnetic systems by means of a Dzyaloshinskii-Moriya (DM) interaction [16,17]. This interaction depends on the DM vector $\vec{D}_{ik}$, associated to the symmetry of the crystal structure. A usual crystalline symmetry group in several materials is the D_n group, where n represents the crystal symmetry. In this symmetry, the interaction energy contribution is proportional to $\vec{m}\cdot(\vec{\nabla}\times\vec{m})$ [13]. A few years ago, Thiaville *et al.* [18] showed that Bloch-like skyrmions are associated with DM vectors $\vec{D}_{ik}$ parallel to $\vec{r}_k-\vec{r}_i$, whereas Néel-like skyrmions are associated with DM vectors $\vec{D}_{ik}$ perpendicular to $\vec{r}_k-\vec{r}_i$.

In this work, we explore the stability of skyrmions characterized by a magnetic texture in between the Néel and Bloch ones. Such magnetic configurations have been recently studied using differential equations and assuming a strong uniaxial anisotropy [19]. Besides they have been addressed as skyrmion-based spin-torque nano-oscillator by Garcia-Sanchez *et al.* [20] and proposed for signal generation and for neuro-inspired applications. These magnetic textures occur naturally because of a competition between DM (chiral behavior) and dipolar (not chiral) interactions [21]. For our study, we consider two DM interactions. In the bulk, we assume that there exists a DM interaction favorable to Bloch-like skyrmions, and at the interface with a substrate, we consider a DM interaction that favors the Néel-like skyrmions. Such DM interactions are due to a break of the inversion symmetry in the bulk, and to the spin-orbit coupling at the interface. Besides, we include the dipolar interaction that plays a role favoring Bloch-like skyrmion. The competition between these three contributions to the energy (interfacial and bulk DM, and dipolar interactions) determines the final state of the system, which may exhibit a complex magnetic configuration. Following these ideas, we study the impact that dipolar energy has in the equilibrium magnetization in an explicit way, as opposed to considering the dipolar energy as an effective anisotropy.

2. Model

For our work we consider a cylindrical dot with radius R and height L ($R \gg L$), coupled to a non-magnetic substrate, as shown in Fig. 1. We assume that the interaction with the substrate occurs in a section of width $t = 0.6$ nm of the dot, as in Ref. [18].

* Corresponding author.
E-mail address: dora.altbir@usach.cl (D. Altbir).

https://doi.org/10.1016/j.jmmm.2019.03.014
Received 13 April 2018; Received in revised form 19 February 2019; Accepted 4 March 2019
Available online 13 March 2019
0304-8853/

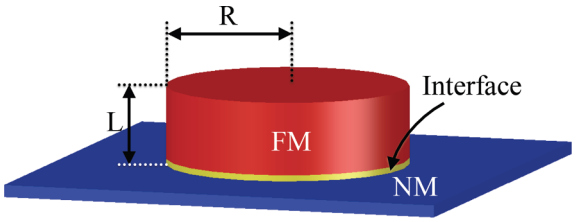

Fig. 1. Schematic representation of the system. The dot, with height L and radius R, has an interface $t = 0.6$ nm with the substrate shown in light grey (yellow online). (For interpretation of the references to colour in this figure legend, the reader is referred to the web version of this article.)

The cylinder has a DM energy due to the symmetry of its crystalline structure defined by a DM constant D_b and interacts with the substrate through a DM interaction determined by a constant D_i. We start by using the explicit expression for the dipolar energy and considering the reduced magnetization $\vec{m}$ as

$$\vec{m} = \sin\Theta\cos\phi_0\,\vec{e}_\rho + \sin\Theta\sin\phi_0\,\vec{e}_\phi + \cos\Theta\vec{e}_z,$$

where $\vec{e}_\rho$, $\vec{e}_\phi$ and are the standard basis in cylindrical coordinates, $\Theta = \Theta(\rho)$ is a function that determines the profile of the z component of the magnetization, m_z, of the skyrmion and ϕ_0 is the helicity [22], as shown in Fig. 2. This parametrization ensures that $|\vec{m}| = 1$ everywhere inside the magnetic dot. If we take $\phi_0 = \nu\pi$ with ν integer, we have a hedgehog or Néel-like skyrmion. On the contrary, we obtain a Bloch-like skyrmion for $\phi_0 = \nu\pi + \pi/2$. Therefore we labeled the states as ϕ_0-twisted-skyrmion, due to the magnetic spiral formed in the cylinder. Concerning the ϕ_0 dependence on z, we used the thin film approximation, a widely used approximation that allows considering the magnetization profile independent of z in sufficiently thin geometries [23].

Assuming exchange, anisotropy, dipolar and DM interactions, the total energy can be written as

$$\begin{aligned} E=\;& E_{\rm ex} + E_{\rm an} + E_{\rm dip} + E^{(b)}_{\rm DM} + E^{(i)}_{\rm DM},\\ E=\;& A\int_V (\vec{\nabla}\cdot\vec{m})^2\,dV - K_u\int_V m_z^2\,dV\\ &+ \tfrac{\mu_0 M_s}{2}\int_V \vec{m}\cdot(\vec{\nabla}U)dV - D_b\int_V \vec{m}\cdot(\vec{\nabla}\times\vec{m})dV\\ &+ tD_i\int_S[(\vec{\nabla}m_z)\cdot\vec{m} - m_z(\vec{\nabla}\cdot\vec{m})]dS, \end{aligned}$$

with A and K_u the stiffness and anisotropy constants, respectively, and D_b and D_i the DM constants in the bulk and at the interface. In this equation M_s represents the saturation magnetization, U corresponds to the magnetostatic potential and the easy axis is along the dot axis. The first two terms of the total energy do not depend on ϕ_0, but the last three contributions to the total energy depend on ϕ_0. After calculating each energy contribution, we obtain

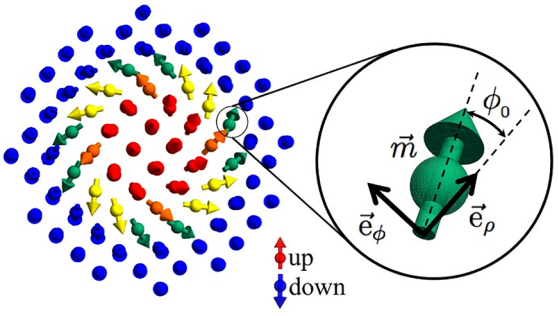

Fig. 2. Magnetization of a twisted-skyrmion and schematic representation of ϕ_0.

$$E = 2\pi LA\int_0^R\left[\left(\frac{d\Theta}{d\rho}\right)^2 + \frac{\sin^2\Theta}{\rho^2}\right]\rho d\rho - 2\pi LK_u\int_0^R\cos^2\Theta\,\rho d\rho + E^{(0)}_{\rm dip} + \alpha_{\rm dip}\cos^2\phi_0 - 2\pi\alpha_{\rm DM}(LD_b\sin\phi_0 + tD_i\cos\phi_0),$$

with $E^{(0)}_{\rm dip}$ denoting the contribution to this energy that does not depend on ϕ_0, and

$$\alpha_{\rm dip} = \mu_0\pi M_s^2\int_0^\infty (Lq + e^{-Lq} - 1)dq\left[\int_0^R \sin\Theta(\rho)J_1(q\rho)\,\rho d\rho\right]^2, \quad (1)$$

and

$$\alpha_{\rm DM} = 2\pi\int_0^R\left[\frac{d\Theta}{d\rho} + \frac{\sin\Theta(\rho)\cos\Theta(\rho)}{\rho}\right]\rho d\rho, \quad (2)$$

depend on the skyrmion profile.

In our calculations, we will consider two expressions for the dipolar energy. In the first case, the dipolar energy is explicitly calculated and then added to the total energy. In the second case, it is considered as a shape anisotropy term and included into the anisotropy constant as $K = K_u + K_{\rm dip}$, with $K_{\rm dip}$ the dipolar anisotropy.

2.1. Skyrmion structure taking full account of the dipolar energy

In this section we consider the detailed calculation of the dipolar energy. Collecting together all contributions to the total energy we can write it as $E = E_0 + E_1[\phi_0]$, with $E_1[\phi_0]$ containing the ϕ_0-dependence of the energy, obtained by adding the DM interactions and the ϕ_0-dependent part of the dipolar interaction. Therefore,

$$E_1[\phi_0] = \alpha_{\rm dip}\cos^2\phi_0 - \alpha_{\rm DM}(tD_i\cos\phi_0 + LD_b\sin\phi_0). \quad (3)$$

The values of ϕ_0 that minimize this expression depend on D_b, D_i, and geometrical parameters, and can be obtained minimizing Eq. (3) with respect to ϕ_0; that is

$$-2\alpha_{\rm dip}\cos\phi_0\sin\phi_0 - \alpha_{\rm DM}(-tD_i\sin\phi_0 + LD_b\cos\phi_0) = 0.$$

By evaluating ϕ_0 minimizing energy in Eq. (3), we notice that Bloch and Néel-skyrmions ($\phi_0 = \pi/2$ or 0, respectively) are formed only when D_i and/or D_b are zero, respectively. If both D_i and D_b are different from zero, a solution with intermediate ϕ_0 is reached.

If we consider the dipolar interaction explicitly, and $D_b = 0$, the equilibrium configuration is a twisted-skyrmion when

$$\frac{\alpha_{\rm DM}}{\alpha_{\rm dip}} < \frac{2}{tD_i},$$

and a Néel-skyrmion otherwise. When $D_i < D_i^c$ (D_i^c is a lower value such as exist skyrmions), the ferromagnetic configuration pointing out-of-plane is a equilibrium configuration. Our study is only in the region $D_i > D_i^c$.

Now we propose an ansatz for the explicit form of the magnetization profile $\Theta(\rho)$. This ansatz has been previously used in several works such as in Refs. [4,24]. We start from the exact solution for a soliton in the non-linear sigma model [25] that gives $m_z(\rho) = (\rho^2 - 1)/(\rho^2 + 1)$. Since this solution is exact on an infinite plane, which is not our case, we introduce a finite size by replacing ρ by $e^{-\lambda(\rho-\rho_0)}$ in $m_z(\rho)$, with λ and ρ_0 as adjustable parameters that are obtained from energy minimization. We propose

$$\Theta(\rho) = -\arccos\left(\tanh\left[\frac{\lambda\rho_0}{R}\right]\right) + \arccos\left(\tanh\left[\frac{\lambda(\rho_0-\rho)}{R}\right]\right),$$

where the first term in this equation is included to avoid energy divergences.

We compare results from our ansatz with results obtained from similar calculations in OOMMF [26], for a cylindrical particle with $t = 0.6$ nm and $R = 50$ nm described by $M_s = 1100$ kA/m, $A = 16$ pJ/m, $K = 0.75$ MJ/m^3 and $L = 3t$. Our ansatz shows a very good agreement with OOMMF results, as illustrated in Fig. 3. In addition, both profiles

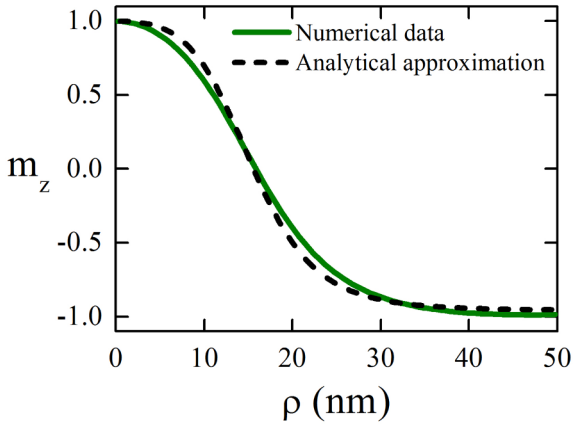

Fig. 3. Magnetic profile for $R = 50$ nm from numerical and analytical calculations. We considered $D_i = 2$ mJ/m^2 and $D_b = 0$. For the analytical profile, we used $\lambda = 7.1$ and $\rho_0 = 13.5$ nm.

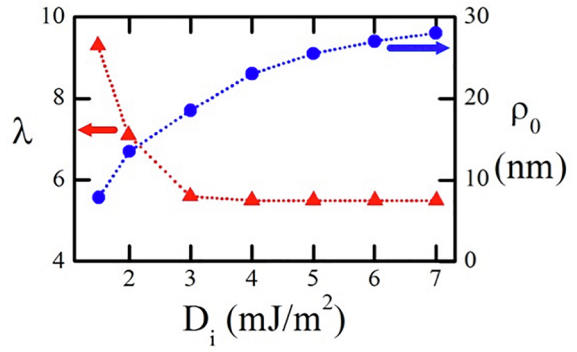

Fig. 4. λ and ρ_0 values that minimize the skyrmion energy from micromagnetic simulations (OOMMF) and $D_b = 0$.

are similar to the one obtained by N. Romming *et. al.* in Ref. [27] with the parameters $w = 16.9$ nm and nm.

Using OOMMF simulations we obtained λ and ρ_0 that minimize the energy. Our results for $D_b = 0$ are shown in Fig. 4. For simplicity we assume λ and ρ_0 independent of D_b. This figure also defines a minimum value of D_i, $D_i^c = 1.5$ mJ/m^2, that allows skyrmion nucleation.

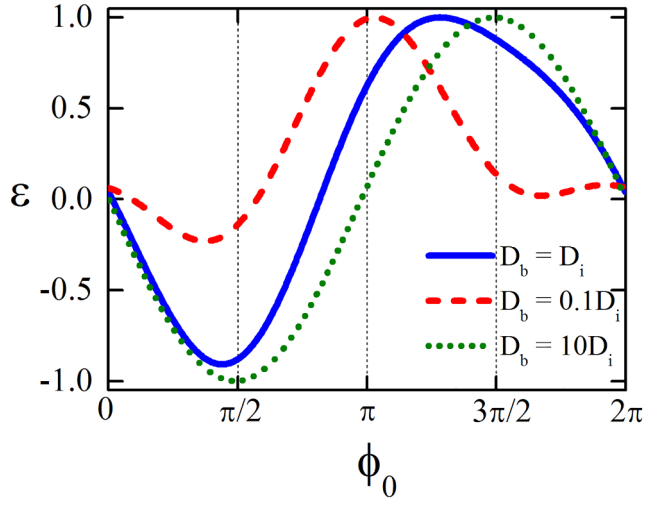

Fig. 5. Normalized energy for a magnetic cylinder with $L = 3t$ and $D_i = 2.0$ mJ/m^2. The solid line illustrates results for $D_b = D_i$, the dashed line represents results for $D_b = 0.1D_i$, and the dotted line corresponds to $D_i = 10D_i$.

Fig. 5 illustrates the behavior of the normalized energy $\varepsilon = E_1[\phi_0]/E_{1,max}$, with $E_{1,max}$ the maximum value for $E_1[\phi]$, as a function of ϕ_0 (see Eq. (3)) for $D_i = 2.0$ mJ/m^2. In this way ε is between -1 and 1. This figure evidence global minima for different D_b values that are related to twisted-skyrmions that appear due to the competition between the dipolar and the DM interactions.

2.2. Skyrmion structure within the shape anisotropy approximation

In this case, the (in-plane) dipolar energy is included as a uniaxial anisotropy term imposing a penalty to the energy if the magnetization points along the z axis. In this case, the ϕ_0 dependence of the approximated dipolar energy disappears. Therefore, only the DM term depends on ϕ_0, and then, from Eq. (3),

$$E_1[\phi_0] = -\alpha_{\rm DM}(R)(tD_i\cos\phi_0 + LD_b\sin\phi_0).$$

In this case, the total energy can be written as

$$\begin{aligned} E &= E_{\rm ex} + E_{\rm an} + E_{\rm DM}^{(b)} + E_{\rm DM}^{(i)}, \\ E &= 2\pi LA\int_0^R \left[\left(\frac{d\Theta}{d\rho}\right)^2 + \frac{\sin^2\Theta}{\rho^2}\right]\rho d\rho \\ &\quad - 2\pi LK\int_0^R \cos^2\Theta\,\rho d\rho \\ &\quad - 2\pi\alpha_{\rm DM}(R)(LD_b\sin\phi_0 + tD_i\cos\phi_0). \end{aligned}$$

If $D_b \neq 0$, the minimization of $E_1[\phi_0]$ gives $\phi_0 = \arctan(LD_b/tD_i)$.

3. Results

Using previous expressions for the energy, we minimize ϕ_0 to obtain the phase diagram for the skyrmions helicity. The stability of the spin configurations obtained with our ansatz has been numerically validated. Starting from the analytical textures for all parameters in the phase diagram, we run the OOMMF code and observe that only very small differences appear in the magnetic configurations.

From Fig. 6 we observe that, for this geometry, Bloch-skyrmion, characterized by $\phi_0 = \pi/2$, are not obtained independent of the dipolar interaction. However, when $D_i = 1.5$ mJ/m^2, a similar structure is obtained defined by $\phi_0 \approx \pi/2$ only when the dipolar interaction is fully considered. From another side, Néel skyrmions need $D_b = 0$. In this case, the full dipolar interaction establishes a lower limit for D_i in order to generate such type of textures, that, when including a shape anisotropy occur for any $D_i > D_i^c$. Finally twisted skyrmions including shape anisotropy occur for any $D_i > D_i^c$ and $D_b \neq 0$, but the inclusion of the full dipolar interaction allows twisted structures also for $D_b = 0$ and D_i values in between D_i^* and D_i^c. In addition, a gap appears in the phase diagram, purely of dipolar origin. This means that some helicities will be never observed for $D_i < D_i^*$, independent of the values of the D_b. An important fact is that when $D_b = 0$ the inclusion of the full dipolar interaction allows the existence of skyrmions with the two chiralities (solid blue line on-line in Fig. 6(a)). For $D_i > D_i^c$ and $D_b \neq 0$ when including dipolar interactions as shape anisotropy the system chooses one of the chiralities, as shown in Fig. 6(b). These results show the importance of including the full dipolar interaction for favoring twisted skyrmion.

Another interesting result is the existence of a critical D_i^* value below which the twisted skyrmion may be stabilized. In our case, $D_i^* \approx 3.0$ mJ/m^2. This effect can be explained by an argument similar to the usual assessment of a mean field second order phase transition. For values of D_i larger than a critical strength, D_i^*, the only minimum of the energy is $\phi_0 = 0$. When D_i reaches D_i^* this solution becomes unstable and two alternative solutions, that break the chirality reversal symmetry, emerge as new global minima. Since, in absence of D_i, the system displays symmetry under chirality reversal, only even powers of ϕ_0 appear in the expansion of the energy function. In the vicinity of D_i^*, i.e. while ϕ_0 can be regarded as small, only a few terms in the expansion need to be taken into account. The second order coefficient changes

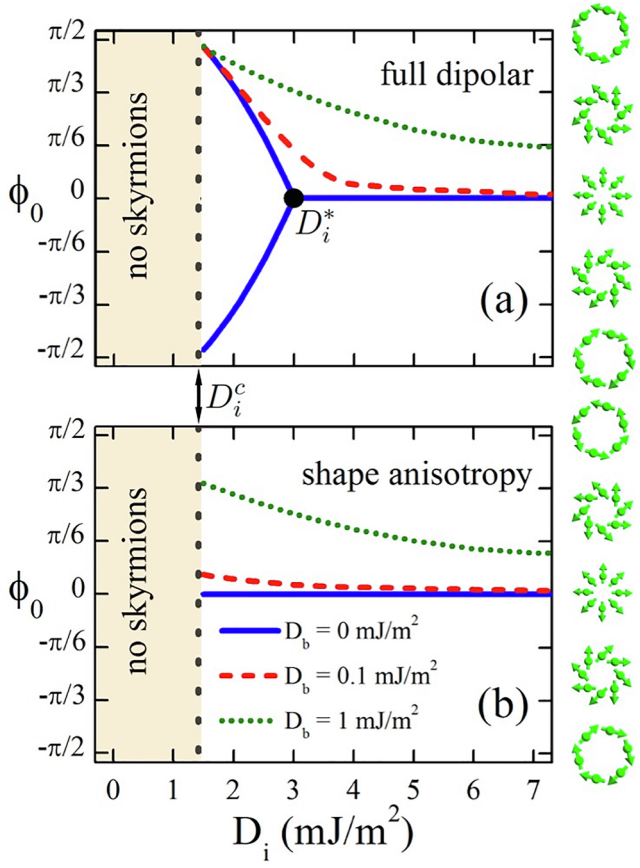

Fig. 6. Stable skyrmion structures as a function of D_i for different values of D_b for a dot with $L = 3t$ when considering (a) full dipolar energy and (b) shape anisotropy. Skyrmions are forbidden in the left zone (beige on-line). In (a) the circular dot represents the critical value D_i^* at which the bifurcation occurs.

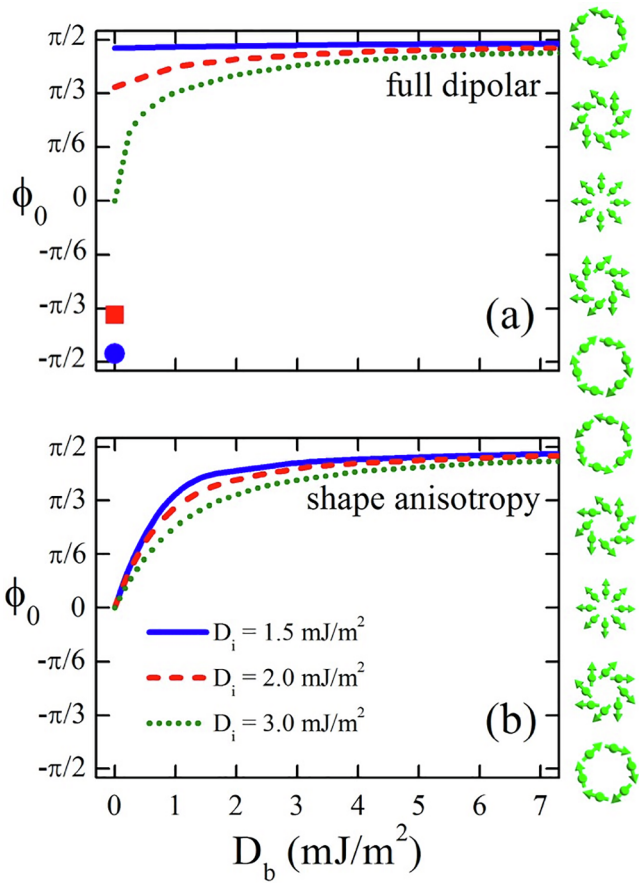

Fig. 7. Stable skyrmion structures as a function of D_b for difference values of D_i for a dot with $L = 3t$ when considering (a) full dipolar energy and (b) shape anisotropy. Square dot corresponds to the stable state with $D_i = 2.0$ mJ/m^2 and circular dot represents results for $D_i = 1.5$ mJ/m^2.

sign as D_i is tuned across D_i^*. This fact is behind the difference in the behavior of the optimal helicity below and above the threshold. Within this approximation, the optimal angle ϕ_0 can be readily shown to scale as $\sim \pm\sqrt{D_i^* - D_i}$. This simple scaling law is, indeed, displayed by the result of the exact calculation in the vicinity of D_i^*.

To clarify the differences between both models, Fig. 7 illustrates the phase diagram for different D_b and D_i values. For $D_b = 0$ and $D_i < D_i^*$ we obtain both negative and positive values of the helicity with a full consideration of the dipolar energy. For $D_b \neq 0$ helicities reach only values higher than zero. In addition, when considering shape anisotropy, ϕ_0 for different D_i can take any positive helicity dependent of the $D_b \neq 0$.

4. Conclusions

In conclusion, in this paper, we have shown that a proper consideration of dipolar interaction leads to skyrmions with a significantly modified internal structure as those obtained with a shape anisotropy contribution. Dipolar interaction favors the generation of twisted skyrmions and, when $D_b = 0$, allows the existence of skyrmions with two chiralities, a very important fact that, otherwise, cannot be observed. The dipolar interaction generates gaps in the phase space, restricting the helicities that can be found in twisted skyrmions. In addition, for $D_b = 0$ our results show the existence of a critical D_i value that allows considering the dipolar interaction as local anisotropy. Our results show the importance of a paper consideration of this interaction, which for simplicity is usually approximated by a shape anisotropy.

Acknowledgement

The authors acknowledge financial support from FONDECYT Grants 1160198, 1150072 and 11170858, Proyecto Basal USA 1555, Grant Dicyt 041831AD, and Financiamiento Basal para Centros Científicos y Tecnológicos de Excelencia (CEDENNA), under project FB0807.

References

[1] A.N. Bogdanov, U.K. Rossler, Phys. Rev. Lett. 87 (2001) 037203.
[2] U.K. Rossler, A.N. Bogdanov, C. Pfleiderer, Nature 442 (2006) 797.
[3] D. Andrikopoulos, Bart Sorée and Jo De Boeck, J. Appl. Phys. 119 (2016) 193903.
[4] K.Y. Guslienko, Z.V. Gareeva, IEEE Magn. Lett. 7 (2016) 7.
[5] S. Woo, K. Litzius, B. Kruger, M.-Y. Im, L. Caretta, K. Richter, M. Mann, A. Krone, R.M. Reeve, M. Weigand, P. Agrawal, I. Lemesh, M.-A. Mawass, P. Fischer, M. Klaeui, G.S.D. Beach, Nat. Mater. 15 (2016) 501.
[6] S. Heinze, K. von Bergmann, M. Menzel, J. Brede, A. Kubetzka, R. Wiesendanger, G. Bihlmayer, S. Blugel, Nat. Phys. 7 (2011) 713.
[7] C. Moreau-Luchaire, C. Moutafis, N. Reyren, J. Sampaio, C.A.F. Vaz, N. Van Horne, K. Bouzehouane, K. Garcia, C. Deranlot, P. Warnicke, P. Wohlhuter, J.-M. George, M. Weigand, J. Raabe, V. Cros, A. Fert, Nat. Nanotech. 11 (2016) 444.
[8] A. Fert, V. Cros, J. Sampaio, Nat. Nanotechn. 8 (2013) 152.
[9] J. Sampaio, V. Cros, A. Fert, S. Rohart, A. Thiaville, Nat. Nanotechn. 8 (2013) 839.
[10] X. Zhang, M. Ezawa, Y. Zhou, Sci. Rep. 5 (2015) 9400.
[11] W. Kang, Y. Huang, C. Zheng, W. Lv, N. Lei, Y. Zhang, X. Zhang, Y. Zhou, W. Zhao, Sci. Rep. 6 (2016) 23164.
[12] Jan Müller, New J. Phys. 19 (2017) 025002.
[13] A. Bogdanov, A. Hubert, J. Magn. Magn. Mater. 138 (1994) 255.
[14] I. Kézsmárki, S. Bordács, P. Milde, E. Neuber, L.M. Eng, J.S. White, H.M. Ronnow, C.D. Dewhurst, M. Mochizuki, K. Yanai, H. Nakamura, D. Ehlers, V. Tsurkan, A. Loidl, Nat. Mater. 14 (2015) 1116.
[15] J.A. Otálora, J.A. López-López, P. Landeros, P. Vargas, A.S. Núñez, J. Magn. Magn. Mater. 341 (2013) 86.

[16] I.E. Dzyaloshinskii, J. Phys. Chem. Solids 4 (1958) 241.
[17] T. Moriya, Phys. Rev. 120 (1960) 91.
[18] A. Thiaville, S. Rohart, É. Jué, V. Cros, A. Fert, Europhys. Lett. 100 (2012) 57002.
[19] A.O. Leonov, T.L. Monchesky, N. Romming, A. Kubetzka, A.N. Bogdanov, R. Wiesendanger, New J. Phys. 18 (2016) 065003.
[20] F. Garcia-Sanchez, J. Sampaio, N. Reyren, V. Cros, J.-V. Kim, New J. Phys. 18 (2016) 075011.
[21] X. Yu, M. Mostovoy, Y. Tokunaga, W. Zhang, K. Kimoto, Y. Matsui, Y. Kaneko, N. Nagaosa, Y. Tokura, PNAS 109 (2012) 8856.
[22] N. Nagaosa, Y. Tokura, Nat. Nanotechnol. 8 (2013) 899.
[23] Z.V. Gareeva, K. Guslienko, Phys. Status Solidi RRL 10 (2016) 227.
[24] N. Vidal-Silva, A. Riveros, J. Escrig, J. Magn. Magn. Mater. 443 (2017) 116.
[25] R. Rajaraman, An Introduction to Solitons and Instantons in Quantum Field Theory, (1987).
[26] M.J. Donahue, D.G. Porter, OOMMF User's Guide, Version 1.2a3 http://math.nist.gov/oommf (2002).
[27] N. Romming, A. Kubetzka, C. Hanneken, K. von Bergmann, R. Wiesendanger, Phis. Rev. Lett. 114 (2015) 177203.